

Quasiparticle spectrum of the cuprate $\text{Bi}_2\text{Sr}_2\text{CaCu}_2\text{O}_{8+\delta}$: Possible connection to the phase diagram

W. Sacks¹, T. Cren¹, D. Roditchev¹ and B. Douçot²

¹*Institut des NanoSciences de Paris, I.N.S.P.,*

Universités Paris 6 et 7, C.N.R.S. (UMR 75 88), 75015 Paris, France and

²*Laboratoire de Physique Théorique et Hautes Énergies, L.P.T.H.E.,*

Universités Paris 6 et 7, C.N.R.S. (UMR 75 89), 75005 Paris, France

(Dated: December 2, 2024)

We previously introduced [T. Cren et al., *Europhys. Lett.* **52**, 203 (2000)] an energy-dependant gap function, $\Delta(E)$, that fits the unusual shape of the quasiparticle (QP) spectrum for both BiSr-CaCuO and YBaCuO . A simple anti-resonance in $\Delta(E)$ accounts for the pronounced QP peaks in the density of states, at an energy Δ_p , and the dip feature at a higher energy, E_{dip} . Here we go a step further: our gap function is consistent with the (T, p) phase diagram, where p is the carrier density. For large QP energies ($E \gg \Delta_p$), the *total spectral gap* is $\Delta(E) \simeq \Delta_p + \Delta_\varphi$, where Δ_φ is tied to the condensation energy. From the available data, a simple p -dependance of Δ_p and Δ_φ is found, in particular $\Delta_\varphi(p) \simeq 2.3 k_B T_c(p)$. These two distinct energy scales of the superconducting state are interpreted by comparing with the normal and *pseudogap* states. The various forms of the QP density of states, as well as the spectral function $A(\mathbf{k}, E)$, are discussed.

INTRODUCTION

A striking feature of the conventional superconducting (SC) state is the small number of parameters needed for its description. With the knowledge of the BCS quasiparticle spectrum, $E_{\mathbf{k}} = \sqrt{\epsilon_k^2 + \Delta_{\mathbf{k}}(T)^2}$, revealing a gap $\Delta_{\mathbf{k}}(T)$ at the Fermi level ($\epsilon_k=0$), the Hamiltonian is basically known and the magnetic, thermodynamic and transport properties can be derived [1]. The gap $\Delta_{\mathbf{k}}(T)$, which vanishes at T_c , is related to the pairing interaction $V_{\mathbf{k},\mathbf{k}'}$ via the BCS self-consistency relation, giving the ratio $2\Delta(0)/k_B T_c = 3.52$, in the weak-coupling isotropic case. It is thus a scalar order parameter of the transition, a fact that has been verified to a high precision [2, 3, 4].

In the case of high- T_c , the probing of the QP spectrum has not led to a solution. Still, a wealth of information on the magnetic field, temperature and doping dependence of the SC state has been obtained [5, 6]. The QP spectral function, as probed using photoemission (ARPES), or the density of states (DOS) as obtained by Scanning Tunneling Spectroscopy (STS), reveal additional singularities which are at odds with a simple BCS d -wave spectrum [7, 8, 9, 10, 11, 12, 13]. In the DOS (Fig. 1, curve 1), the QP peaks (P) are very pronounced and are followed by a dip feature (D) at higher energy (at $E = E_{dip}$). Although the origin is still debated, there is some strong-coupling effect on the quasiparticles : a self-energy is implied [14, 15, 16, 17, 18]. A mean-field approach is insufficient in the context of correlated electrons [19, 20], coupled spin-charge degrees of freedom [21, 22, 23], phase fluctuations [24, 25, 26], or a competing order [27, 28, 29, 30]. Thus the SC state can no longer depend on one parameter.

The main question addressed in this work is can the QP spectrum still be described in simple terms (eg. in an extended BCS way) and if so, how does it reflect the order parameter? To answer, the details of the

quasiparticle DOS must be understood. As we showed in ref. [11], the particular shape of the measured spectrum, illustrated by curve 1, cannot be obtained from a simple mean-field gap, giving curve 3. However, our resonant gap function $\Delta(E)$, described further in Sec. I, nicely fits the variety of spectra published since [12, 13, 31, 32, 33, 34, 35, 36, 37, 38, 39, 40]. Despite a number of analyses of the QP spectra, taking into account the coupling to a collective mode [17, 22, 31, 32, 41, 42, 43, 44], the effect of van Hove singularities or the particle-hole asymmetry [33, 45, 46, 47], the effects of disorder or phase fluctuations [18, 21], the spectrum 1 is difficult to derive.

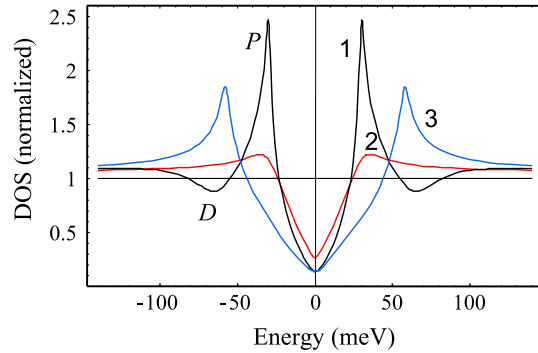


Fig. 1: Curve 1 - Quasiparticle DOS as observed by tunneling showing pronounced peaks at $E = \pm \Delta_p$ followed by dips. Curve 2 - *Pseudogap* type spectrum observed in the vortex core, or for $T \geq T_c$. Curve 3 - Extended BCS (d -wave) DOS, but with a larger gap. All three are generated by our gap function, Eq. (10).

The physical parameters of a self-energy, or equivalent gap function, have yet to be connected to the phase diagram. Important leads on the spectral function (or DOS), as a function of doping and temperature, have been obtained using ARPES and tunneling. First, a well-defined QP peak at the position Δ_p (our

notation) develops in the SC state and is of d -wave symmetry [48, 49, 50, 51, 52]: $\Delta_{\mathbf{k}} \propto \Delta_p \cos(k_x - k_y)$, yielding the characteristic V shape in curves 1 - 3. However, the ratio $2\Delta_p/k_B T_c$ widely departs from the BCS value; Δ_p decreases roughly linearly with p , with a large negative slope, from underdoped to overdoped sides of the phase diagram [6, 9, 49]. As is well established, $T_c(p)$ is dome shaped with a maximum at $p_0 \simeq .16$, where $T_c \simeq 95$ K, for $\text{Bi}_2\text{Sr}_2\text{CaCu}_2\text{O}_{8+\delta}$. Thus, the position of the QP peak (at $E = \Delta_p$) is not the energy scale the global SC order parameter.

The QP spectrum has been probed as a function of rising temperature [9, 49, 50, 51, 52, 53, 54]. Above T_c , instead of revealing the normal state with a metallic DOS, the spectrum displays a pronounced but peakless gap of width $2\Delta_{PG}$ at the Fermi level. This *pseudogap*, see curve 2, disappears at the higher temperature T^* , and has possibly the same angular dependence as $\Delta_{\mathbf{k}}$. Moreover, Δ_p and Δ_{PG} have approximately the same magnitude [49, 53, 54]. One finds that $\Delta_p \approx 3k_B T^*$, so $T^*(p)$ follows the identical trend as Δ_p in the phase diagram. The challenge is to understand three contiguous phases (superconducting, pseudogap and normal). However, the $T^*(p)$ curve on the overdoped side, where the data is rare, is the subject of hot debate [6, 20, 26, 30], in particular whether or not it crosses the $T_c(p)$ dome. The T^* inferred from NMR Knight shift, resistivity and specific-heat measurements may correspond to still a higher temperature, such as the onset of anti-ferromagnetic fluctuations, distinct from the vanishing of Δ_{PG} as observed by ARPES [55].

The origin of the pseudogap is a key question about high- T_c , and is still highly controversial. Theories fall into two qualitative categories: Δ_{PG} is either a precursor to, or competes with, the SC state [56]. The first [24, 26, 56] is immediately compelling due to the phase diagram: below T^* incoherent pairs are formed (thus the pseudogap) and condense at T_c . It also follows many aspects of the SC state (low carrier density, strong coupling energy, small coherence length, sensitivity to disorder, etc.) and is theoretically tractable [24, 56, 57, 58]. In the second category, the competing order (charge or spin density wave, Varma currents, RVB,...[19, 27, 28, 29]) sends T^* down, possibly across the T_c dome, to a quantum critical point above which a new phase is formed. Deciding between these two categories would be a significant advance.

Conductance mapping using STS has provided valuable information. The ‘normal’ state found within the vortex core [12, 59] reveals a pseudogap analogous to the one found just above T_c [54]. The local vanishing of the SC order parameter in a vortex core is due to the phase singularity; but contrary to the conventional case, the pseudogap persists. We found a quasi-identical pseudogap, in zero magnetic field, caused by weak disorder [60]. In both cases, Δ_p and Δ_{PG} have about the same magnitude [12, 39, 59, 60, 61]. Thus an important constraint on the SC gap function is its

smooth transition to the peak-less pseudogap when phase coherence is lost: curve 1 \rightarrow curve 2 (Fig. 1).

Nozières and Pistolesi [62] have described a superconducting state when a precursor gap, such as Δ_{PG} , is initially present. However, their model implies that the SC gap must be larger than the precursor gap. Thus, given curve 2 for the pseudogap, curve 3 is expected in the superconducting state, not curve 1. Moreover, the high spectral weight of the QP peaks (curve 1) leads to an apparent paradox: electronic states seem to move towards the Fermi level in the transition to the SC state [63]. Any complex self-energy or gap function must give the correct energy change for the pseudogap to SC transition.

The situation becomes complex in the case of strong disorder: local STS mapping has revealed pseudogap/SC gap variations at the surface of BSCCO [34, 35, 40, 61]. Clearly, in this case, there are changes of both SC amplitude and phase [21, 57, 64, 65, 66]. In Pb-substituted BSCCO the disorder causes ‘superconducting’ islands to form [61], where the intensity of the spectral fine structure correlates with the degree of long-range order. Recent theoretical work by Atkinson [21] and experimental STS by Fang et al. [40] corroborate this conclusion. Even if the inhomogeneity is not an intrinsic property [6, 37, 67], the cuprate SC state is sensitive to local perturbations [64, 65, 66], and the attenuation of the spectral fine structure is a clear sign. Then, several parameters are needed for the interpretation of the tunneling DOS.

In this Article, we analyze the QP spectrum, $E_{\mathbf{k}}$, as inferred from the sharpest tunneling DOS of BSCCO. The detailed DOS shape (pronounced QP peaks, followed by dips at higher energy) is due to a single resonance in our energy-dependant gap function, Section I. Such a resonance in the QP spectrum is possibly the coupling to a collective mode [15, 17, 31, 32, 41, 42, 43] of the same origin as the resonance seen using inelastic neutron scattering [68] and which scales with T_c : $\Omega \sim 5.3 k_B T_c$. Zasadzinsky et al. studied the dip position as a function of doping using strong-coupling theory [13], and suggested that the dip energy is also related to T_c . Since the origin of the resonant gap function (or QP self-energy) is still unknown, our aim is to show how the basic parameters depend on the carrier density p . In Sec. II we find that one of the energy terms, Δ_{φ} , is compatible with an order parameter: it is proportional to $k_B T_c(p)$. The predicted shape of the QP density of states is then studied as a function of p . We treat the transition to the PG state (Sec. II), and the role of the two distinct energy scales (Sec. III). Finally, the QP spectral function and self-energy are discussed (Sec. IV).

I. SUPERCONDUCTING GAP FUNCTION

Here the quasiparticle DOS, having the essential characteristics of the observed STS conductance spectra, is derived. In Fig. 2, we show such a spectrum obtained on BSCCO, near optimally doped, from our group (2a) which is compared to (2b), a spectrum from Pan, Hudson et al. [12]. One can again see the pronounced QP peaks, the steep slope on the outer side of each peak, followed by the dip feature previously described. In this Section, we focus on these main aspects of the DOS; the questions of the background slope (as in Fig. 2b), the Fermi surface anisotropy, the particle-hole asymmetry and the van Hove singularity, have already been given extensive treatment [33, 46, 47, 69, 70]. The detailed fits of Fig. 2, solid lines, give the key parameters of our SC gap function, without such considerations.

Expression for the QP-DOS

Consider the spectral function, as measured by ARPES [7, 8, 49, 50, 51, 52, 53, 63], in the two-dimensional model with $\vec{k} = (k, \theta)$ the wave vector in the *ab* plane :

$$A(\mathbf{k}, E) = \frac{1}{\pi} \operatorname{Im} G(\mathbf{k}, E) \quad (1)$$

where $G(\mathbf{k}, E)$ is the single-particle Green's function. The superconducting DOS is then [17, 71] :

$$N_s(E) = \sum_{\mathbf{k}} A(\mathbf{k}, E)$$

which is measured in the tunneling experiment. Converting sums to integrals in the usual way :

$$N_s(E) = \frac{N_n(0)}{2\pi} \int_0^{2\pi} d\theta \int_{-\infty}^{\infty} d\epsilon_k A(\mathbf{k}, E) \quad (2)$$

where ϵ_k and $N_n(0)$ are the normal excitation spectrum and Fermi-level DOS, respectively. This expression ignores the effect of the Fermi surface anisotropy [46, 69]. In the case of an ideal quasiparticle with zero lifetime broadening, and dispersion $E_{\mathbf{k}} = \sqrt{\epsilon_k^2 + \Delta_{\mathbf{k}}^2}$, the propagator is [3, 71] :

$$G(\mathbf{k}, E) = \frac{u_k^2}{E - E_{\mathbf{k}} + i0^-} + \frac{v_k^2}{E + E_{\mathbf{k}} + i0^-}$$

with u_k, v_k the usual coherence factors. Then, $A(\mathbf{k}, E)$ is just: $A(\mathbf{k}, E) = u_k^2 \delta(E - E_{\mathbf{k}}) + v_k^2 \delta(E + E_{\mathbf{k}})$ where each term corresponds to a quasiparticle added ($E > 0$) or removed ($E < 0$), respectively.

For example, with fixed $E > 0$, the integral in (2) picks up two poles at $\pm\epsilon_k$ of amplitude $u_k^2(-\epsilon_k)$ and $u_k^2(+\epsilon_k)$. As is well known [3, 71], the coherence factors disappear in the symmetric case, since $u_k^2(-\epsilon_k) + u_k^2(+\epsilon_k) = 1$. We shall thenceforth ignore them, and consider for both tunneling and ARPES

that the values $\pm\epsilon_k$ are equivalent. Using Eq. (2) the expected result is obtained :

$$N_s(E) = N_n(0) \frac{1}{2\pi} \int_0^{2\pi} d\theta \left(\frac{\partial \epsilon_k}{\partial E_{\mathbf{k}}} \right)_{E_{\mathbf{k}}=E} \quad (3)$$

It is then convenient to define the partial (one dimensional) DOS at the angle θ :

$$N_s(E) = \int_0^{2\pi} n_s(E, \theta) d\theta \quad (4)$$

and, in the extended BCS *d*-wave model [69, 72], the partial DOS is :

$$n_s(E, \theta) = \frac{N_n(0)}{2\pi} \frac{E}{\sqrt{E^2 - \Delta_p^2 \cos^2(2\theta)}} \quad (5)$$

Expressions (4, 5) can be used to generate the curve 3 in Fig. 1 which, as we have stressed, fails to match the strong spectral weight of the QP peaks, and the dip features, obvious in the experiments (Fig. 2). In the general case, beyond the mean-field approach, one must evaluate :

$$n_s(E, \theta) = \frac{N_n(0)}{2\pi} \int d\epsilon_k A(\mathbf{k}, E) \quad (6)$$

assuming a suitable model for $A(\mathbf{k}, E)$ [14, 17, 18, 22, 32, 42].

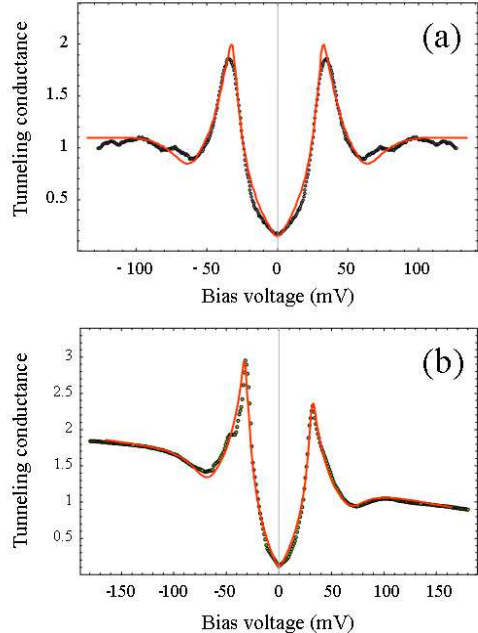


Fig. 2 : Dotted lines - local STS conductance spectra. Solid lines - fits using the model (9, 10).

(a) Symmetrized spectrum from ref. [11], with background removed. Here $\Delta_p = 31.5$ and $E_{dip} = 64$ are fixed; the two free parameters are: $\Delta_{\varphi} = 18.5$ and $E_0 = 50$, all in meV. Also, $E_0 = \Delta_0$, $\eta = \Delta_{\varphi}$ and $A=2$, as seen in Fig. 3. The broadening values are $\Gamma = .08 \Delta_p$ and $\delta = 0.1$.

(b) Spectrum from Pan et al. [12]. The gap function (10) is used but the parameters, $\Delta_p(p)$ and $\Delta_{\varphi}(p)$, are from the

p -dependent fit to the data (Fig. 4a). The best fit is for $p = .175$, with the background slope added. All parameters are nearly identical with (a) except $E_0 \simeq 1.06 \Delta_0$ and $\Gamma = .03 \Delta_p$.

Our approach is to consider that strong-coupling modifies the electron-electron interaction, but *without the retarding effects* that would occur in the case of phonon-mediated pairing [11]. Thus we write $\Delta_{\mathbf{k}} \rightarrow \Delta_{\mathbf{k}}(E_{\mathbf{k}})$, and the new dispersion law is :

$$E_{\mathbf{k}} = \sqrt{\epsilon_k^2 + \Delta_{\mathbf{k}}(E_{\mathbf{k}})^2} + i\Gamma \quad (7)$$

where we add Γ , the lifetime broadening introduced by Dynes [73]. Assuming particle-hole symmetry, one can use :

$$A(\mathbf{k}, E) = \frac{1}{\pi} \operatorname{Im} \frac{1}{E - E_{\mathbf{k}} + i0^-} \quad (8)$$

and, performing the complex integration in (6), we obtain for the partial DOS :

$$n_s(E, \theta) = \frac{N_n(0)}{2\pi} \operatorname{Re} \frac{E - i\Gamma - \Delta_{\mathbf{k}}(E) \frac{\partial \Delta_{\mathbf{k}}(E)}{\partial E}}{\sqrt{(E - i\Gamma)^2 - \Delta_{\mathbf{k}}(E)^2}} \quad (9)$$

Here $\Delta_{\mathbf{k}}$, evaluated at the pole ($E_{\mathbf{k}} = E$), is a function of θ . For a constant gap $\Delta_{\mathbf{k}} = \Delta_p$, we get back Dynes's formula for the BCS DOS with the lifetime broadening. In the general case, (9) is the basic equation for the quasiparticle DOS in our approach, once integrated over θ . It contains a new term in the numerator, $-\Delta_{\mathbf{k}} \partial \Delta_{\mathbf{k}} / \partial E$ which is responsible, as already shown in [11], for the distinct modification of the DOS seen in Fig. 2. It can be used to match the tunneling data of [9, 10, 11, 12, 13, 34, 35, 36, 37, 38, 39, 40, 60, 61, 69, 70].

Superconducting gap function

We now consider the particular gap function appropriate for fitting the data (solid lines in Fig. 2). For the superconducting state, we have made a slight change in notation with respect to ref. [11]. Assuming $\Delta_{\mathbf{k}}(E) = \cos(\theta)\Delta(E)$, the gap function along the anti-nodal direction is now written :

$$\Delta(E) = \Delta_p + \Delta_{\varphi}(1 - g(E)) \quad (10)$$

where Δ_p and Δ_{φ} are constant parameters and $g(E)$ is a simple Lorentzian :

$$g(E) = A \frac{\eta^2}{(E - E_0)^2 + \eta^2} \quad (11)$$

having the standard parameters. Thus the second term in (10) is an anti-resonance (a local decrease in the pair potential). It provokes an additional peak, and dip, in the DOS near the two possible extrema of $dg(E)/dE$ (see upper panel, Fig. 3).

Consider the problem of fitting the DOS in some systematic way: there are *a priori* 5 parameters (the

role of Γ will be discussed subsequently). We commence with the data of Fig. 2a, where the spectrum is symmetrized and the background removed. From our previous work [11], the resonance energy must lie between the QP peaks and the dip position; an estimate is $E_0 \sim (\Delta_p + E_{dip})/2$. This condition ensures that the QP peaks are reinforced, where the extremum of $-d\Delta/dE$ is positive, and gives the dip at a higher energy, where $-d\Delta/dE$ is a negative extremum (see Fig. 3).

Since Δ_p is *defined* as the QP peak position, easily estimated from the data, we have the further condition that: $\Delta(\Delta_p) = \Delta_p$, also illustrated in Fig. 3. Using (10) and (11), this gives $g(\Delta_p) = 1$, or :

$$A = 1 + \frac{(E_0 - \Delta_p)^2}{\eta^2} \quad (12)$$

as a constraint on the parameters. A second constraint is found by writing the dip position, E_{dip} , using the analytical expression of the DOS. Considering the extremum of $\Delta d\Delta/dE$ leads to the good approximation : $E_{dip} \simeq E_0 + .73\eta$. Therefore, taking E_{dip} and Δ_p to be known, the fit to the spectrum of Fig. 2a can be done by the variation of only two free parameters: E_0 and Δ_{φ} . Their final values determine the precise concavity in the DOS, between the QP peak energy and E_{dip} , which is *a priori* unknown.

For the fit of spectrum 2a, using $\Delta_p = 31.5$ and $E_{dip} = 64$, we obtain the values $E_0 = 50$, and $\Delta_{\varphi} = 18.5$, all in meV. The problem is thus simplified by the following outcome: $E_0 = \Delta_p + \Delta_{\varphi} = \Delta_0$, with $\eta = \Delta_{\varphi}$ and $A=2$.

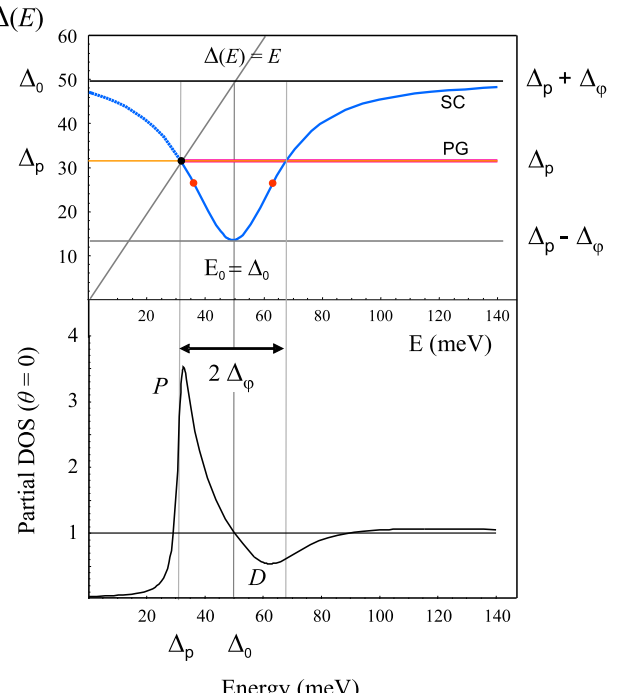


Fig. 3 : Characteristics of the SC gap function and their link to the DOS along the anti-nodal direction ($\theta = 0$).

Upper panel - Real part of $\Delta(E)$ from the fit of spectrum Fig. 2a. Note the anti-resonant shape, with the minimum

at the energy $E_0 = \Delta_0$, while both amplitude and width are $2\Delta_\varphi$. The intersection point, $\Delta(E) = \Delta_p$, gives the QP peak at Δ_p . For large energies, the pairing interaction, is $\Delta(E) \simeq \Delta_0 = \Delta_p + \Delta_\varphi$.

Lower panel - Partial DOS showing a sharp QP peak (P), followed by the dip (D) at the higher energy E_{dip} . The derivative of the gap function, as in Eq. (9), reinforces the quasiparticle peak (negative extremum) and causes the dip feature (positive extremum).

The corresponding function $\Delta(E)$ is depicted in the upper panel of Fig. 3, with the partial DOS along $\theta = 0$ for direct comparison (lower panel). One can see that $\Delta(E)$ has a minimum at $E_0 = \Delta_0$, where its value is $\Delta_p - \Delta_\varphi$, then it increases towards the asymptotic value $\Delta_p + \Delta_\varphi$, when $E \gg E_{dip}$. Note that the total amplitude of the resonance, $2\Delta_\varphi$, is identical to its width. In short, we obtain :

$$\Delta_0 - \Delta_p = E_0 - \Delta_p = \eta = \Delta_\varphi ,$$

and we propose that these relations should scale when the carrier density, p , varies (Section II). The dip position, near to $\Delta_p + 2\Delta_\varphi$, is more precisely :

$$E_{dip} \simeq \Delta_0 + .73 \Delta_\varphi \simeq \Delta_p + 1.73 \Delta_\varphi$$

so that $E_{dip} - \Delta_p \propto \Delta_\varphi$. The latter parameter thus plays a fundamental role in our model.

Broadening parameters

Two broadening parameters in the final fits of Fig. 2 are used. First, the $i\Gamma$ introduced by Dynes to treat a finite quasiparticle lifetime, artificially displaces the pole in the spectral function (8) off the real axis. It is equivalent to a Lorentzian broadening of the DOS, of full-width $\sim 2\Gamma$, affecting the states at all energies. Consequently, in the lower panel of Fig. 3, virtual states lie within the gap of the partial DOS (for $E < \Delta_p$). As we discuss in a recent paper [74], several factors can contribute to Γ both intrinsic (inelastic scattering, many-body effects,...) and extrinsic (high-frequency noise,...). In Fig. 2, the Γ value was adjusted to fit the zero-bias conductance.

The QP peaks, as calculated using (10), are initially higher than those of Fig. 2. Since Γ is fixed, a second broadening parameter is introduced: we replace Δ_p by a complex number with a small imaginary part, $\Delta_p \rightarrow \Delta_p(1 - i\delta)$. This has a major effect on the QP peaks, but a small one on the remaining spectrum. Intuitively, the imaginary part represents a smearing of the value of Δ_p , such as in the case of gap anisotropy [74] or Doppler shifts due to supercurrents [75]. While this ansatz is used to model the pseudogap in Section II, it has a negligible influence on the fit parameters deduced here.

II. CONNECTION TO THE PHASE DIAGRAM

The fit to the BSCCO spectrum, Fig. 2a, leads to the simple result that the width, amplitude and position of the anti-resonance are all simply related to

the quantity Δ_φ ; assuming Δ_p to be known. The QP spectrum therefore depends on only *two* energy scales. This section is devoted to their possible link to the phase diagram: we infer how the parameters of the SC gap function change with the carrier density.

Doping dependance of the energies

The foregoing suggests that Δ_φ must have a new meaning. Consider the asymptotic value of $\Delta(E)$ for large E : $\Delta(E) \simeq \Delta_p + \Delta_\varphi = \Delta_0$ for $E \gg E_{dip}$ (Fig. 3). $\Delta(E)$ is then constant up to some higher cut-off energy, as in BCS theory. Along the anti-nodal direction : $E_{\vec{k}} \approx \sqrt{\epsilon_{\vec{k}}^2 + \Delta_0^2}$, and Δ_0 is thus interpreted as the *total spectral gap* in the SC state, even though the QP peak remains at the smaller energy Δ_p . The pseudogap in the vortex core [12, 39, 59], where phase coherence is lost, takes on a value $\Delta_{PG} \simeq \Delta_p$ and, aside from the thermal broadening, the same holds for the pseudogap just above T_c [49, 53, 54].

We now suggest that Δ_φ is tied to the condensation energy. The energy (per pair) of the SC state is then $\sim -\Delta_\varphi$, with respect to the PG state, but it is $\sim -\Delta_0$ with respect to the normal state. As will be discussed in Sec. III, the integration over energy states, involving the full $\Delta_{\mathbf{k}}(E_{\mathbf{k}})$, is necessary to obtain the precise energy changes.

We can thus put : $\Delta_\varphi = C k_B T_c$ where C is to be determined. From the fit of Fig. 2a, using $T_c \simeq 90$ K, and $\Delta_\varphi = 18.5$ meV, gives $C \simeq 2.4$.

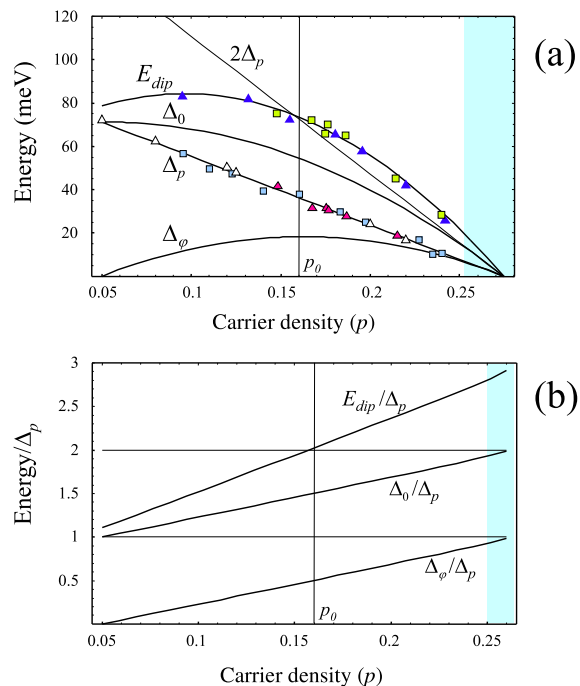


Fig. 4. Doping dependence of the two basic parameters of the gap function, $\Delta_p(p)$ and $\Delta_\varphi(p)$, their sum, $\Delta_0(p)$, and the dip position E_{dip} .

Upper panel (a) - $\Delta_p(p)$ line : Linear fit to the QP peak positions taken from ARPES data [8, 49, 53], SIS/SIN tunneling [9, 13, 31, 32], and STM [10, 11, 12, 36, 37, 69]. E_{dip} line : Best quadratic fit to the dip position, as estimated from STM data [10, 11, 12, 36, 37, 69] and

SIS tunneling [9, 13, 32]. The solution of the fit gives $\Delta_\varphi(p) = 2.3 k_B T_c(p)$ and $E_0 = 1.06 \Delta_0(p)$.

Lower panel (b) - Analogous diagram to (a) but with parameters *normalized* to the gap energy Δ_p : simple linear laws are obtained, Eqs. (14-16). The principal energy scale of the SC state, and determining the DOS fine-structure, is $\Delta_\varphi(p)$. No evidence for a critical point is seen for $0.05 < p < 0.25$.

With this result, one could use scaling arguments to infer the behavior of the parameters as a function of p . However, in view of the dispersion of the tunneling and ARPES data, using a single spectrum and one value of T_c is restrictive. We take a different approach by first plotting in Fig. 4a a larger set of data of the QP peak position, Δ_p . Assuming that the critical temperature $T_c(p)$ is known [6], one can deduce the linear behavior of $\Delta_p(p)$ by a quadratic fit [9]. The data are from the SIS (SC-vacuum-SC) break junction [9, 13, 31, 32], which probes the electronic structure deep in the sample; SIN tunneling data, as well as ARPES data, are included [8, 49, 53]. The dip position (E_{dip}), as seen in many different tunneling experiments [9, 10, 11, 12, 13, 32, 36, 37, 69], is also plotted in Fig. 4a. The points evidently follow a continuous curve throughout the phase diagram. We propose to find this curve via a best quadratic fit using the gap function, which fixes all the parameters.

The two energy terms are thus $\Delta_p(p)$ and $\Delta_\varphi(p) = C k_B T_c(p)$ where the best value of C is to be determined. In order to calculate E_{dip} we could use the previous condition $E_0 = \Delta_0$, which led to $E_{dip} \simeq \Delta_p + 1.73 \Delta_\varphi$. However, the spectrum Fig. 2b, from Pan et al., cannot be precisely fit with the resonance energy exactly at Δ_0 . This is the essential difference between the two spectra (2a and 2b); the latter dip position is slightly at a higher energy.

From our study of YBCO in [11], we noticed the resonance energy can be larger than Δ_0 . We thus write $E_0 = \lambda \Delta_0$, in the general case, and determine the value of λ at the same time as C . The expression for the dip energy is then :

$$E_{dip} = \lambda \Delta_0 + .73 (\lambda \Delta_0 - \Delta_p) \quad (13)$$

and all other parameters retain their previous meaning. Putting $\Delta_p(p)$ and $\Delta_\varphi(p) = C k_B T_c(p)$ in (13), and fitting the data of Fig. 4a, yields: $C = 2.3$, $\lambda = 1.06$, and the continuous curve $E_{dip}(p)$. The two values differ by about 5% from the single-point estimate and, considering the uncertainty in the data, the earlier observation in [11] that $E_0 \sim \Delta_0$ is maintained. More significantly, we find that $\Delta_\varphi(p) = 2.3 k_B T_c(p)$ is consistent throughout the phase diagram, from underdoped to overdoped sides.

In Fig. 4a the total spectral gap $\Delta_0(p)$, and the amplitude $\Delta_\varphi(p)$, are plotted as a function of p . One observes that $\Delta_\varphi(p)$ merges smoothly with $\Delta_p(p)$ on the overdoped side. Consequently, $\Delta_0(p)$ is a smooth convex function of p ranging from Δ_p to $2\Delta_p$. Extrapolating $E_{dip}(p)$, it varies from $\sim \Delta_p$ to $\sim 3\Delta_p$ in the

same range of p . At optimal doping, $p = p_0$, the values are $\Delta_\varphi \simeq \Delta_p/2$ and $\Delta_0 \simeq 3\Delta_p/2$. The dip position is at $E_{dip} \simeq 2\Delta_p$, in agreement with ref. [13].

Simple trends are found by plotting the parameters as ratios with respect to Δ_p , Fig. 4b. We see that Δ_φ/Δ_p , Δ_0/Δ_p and E_{dip}/Δ_p are increasing linearly as a function of p . Moreover, if we write p as the *excess* carrier density from the minimum value of .05, i.e. the doping at the SC onset, we obtain :

$$\frac{\Delta_\varphi}{\Delta_p} \simeq \frac{p}{2p_0} \quad (14)$$

$$\frac{\Delta_0}{\Delta_p} \simeq 1 + \frac{p}{2p_0} \quad (15)$$

$$\frac{E_{dip}}{\Delta_p} \simeq 1.1 + \frac{0.9p}{p_0} \quad (16)$$

where $p_0 \simeq .11$ is the optimal doping. The first two are obtained from the Taylor expansion of Δ_φ/Δ_p while the third is from Eq. (13), using the value $\lambda = 1.06$. Thus E_{dip}/Δ_p shows nearly twice the slope as Δ_φ/Δ_p , and varies from about ~ 1 to ~ 3 in the complete doping range.

Such a straightforward relationship between the parameters was not expected. If Δ_φ is indeed the ‘condensation amplitude’, it continuously increases relative to the precursor gap, Δ_p , throughout the phase diagram. Since the latter decreases linearly with doping, the order parameter is parabolic shaped :

$$\Delta_\varphi = \frac{p \Delta_p(p)}{2p_0} \simeq 2.3 k_B T_c(p) \quad (17)$$

With the previous hypotheses, Eq. (17) expresses a new precise relation between the QP peak positions and the order parameter of the SC transition.

To conclude the discussion on the results from the fits, it is remarkable that the gap function, $\Delta(E)$, as displayed in Fig. 3, scales perfectly as a function of p through the variation of its amplitude, Δ_φ , and the resonance energy, $\lambda \Delta_0$. As with refs. [9, 13], we find no abrupt change in the QP spectrum, nor in its underlying parameters, while spanning the carrier concentration. We conclude that a critical point, if there is one, is situated at the right end of the T_c dome.

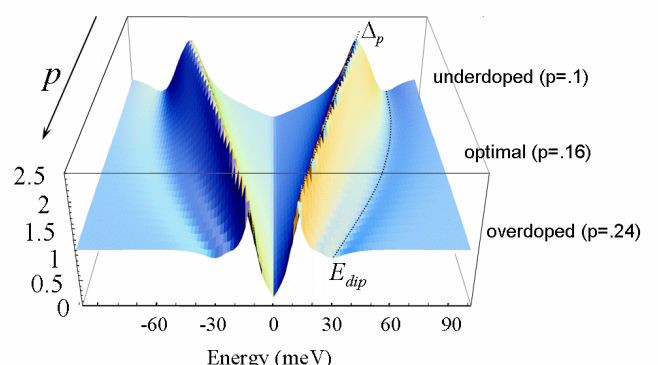


Fig. 5. Plot of the quasiparticle DOS evolution as a function of p , the carrier density. The values of the parameters

used in the gap function are fixed from Fig. 4a: the QP peaks (Δ_p) follow a linear trend, while the dip position, E_{dip} , lies along the curve given by (16). The difference between the dip and the peak positions is $\sim 2\Delta_\varphi(p)$. Note the detailed DOS shape, varying significantly from underdoped to overdoped sides.

Shape of the quasiparticle DOS

The gap function $\Delta(E)$ is now uniquely determined for the range of carrier concentration of interest ($.1 < p < .24$). It is then possible to fit the QP DOS with essentially one free parameter (p), aside from the broadening and the background slope. The spectrum of Fig. 2b, from Pan et al., was fitted by adjusting the value of p , the final value being $p = 0.175$ (see Fig. 5). This could be an approximate measure of the local value of the doping at the surface of the sample, but the background slope adds some uncertainty. Our objective here was mainly to reduce, as far as possible, the number of free parameters.

The variation of the QP DOS shape as a function of p is shown as a surface plot in Fig. 5. As expected, the peak position follows a linear law, while the dip follows the curve given by

$$E_{dip} \simeq 1.1\Delta_p(p) + 1.8\Delta_\varphi(p)$$

as a direct consequence of the gap function (10). The detailed shape of the QP DOS is not the same on each side of optimal doping due to the relative position of Δ_0 compared to Δ_p . Indeed, on the extreme underdoped side, where $\Delta_p > \Delta_\varphi(p)$, the outer slope of the QP peaks is more rounded, with a slight negative concavity between peak and dip. On the overdoped side, $\Delta_p \simeq \Delta_\varphi(p)$, the DOS has sharper peaks and dips, but also a positive concavity between them. A closer look at the extreme overdoped case reveals a new singularity, near Δ_0 (a small kink). The kink is due to a new extremum of $d\Delta(E)^2/dE$, but this prediction remains to be verified experimentally.

The question as to whether we obtain ‘BCS behavior’ on the overdoped side can be addressed. In one sense we do: this limit gives $\Delta_p(p) \simeq \Delta_\varphi(p) \simeq 2.3 k_B T_c$ and a single parameter is then tied to T_c . However, the total spectral gap Δ_0 becomes twice too large ($\sim 2\Delta_p$) so that the dip still persists, near $\sim 3\Delta_p$, which contradicts the BCS d -wave case. Thus, the precursor gap maintains its influence when $p \rightarrow 2p_0$. In fact, the results of Figs. 4 and 5 clearly show that the gap function is non BCS-like throughout the whole phase diagram.

Our model allows an order of magnitude for the value of T^* , defined by the vanishing of the precursor gap. Using the data of [8, 49, 53], we find roughly that $2.8 k_B T^* \simeq \Delta_p$. Combined with Eq. 14, we get:

$$T^* \simeq 1.6 (p_0/p) T_c$$

assumed valid for $T^* \geq T_c$. It follows that the two temperatures merge at $p = 1.6 p_0 \simeq .18$, perhaps remaining merged for $p > 1.6 p_0$, but this is an open question. Note that the excess doping level at the (T^*, T_c) crossing point is $.18$, while the absolute level is $.23$, i.e. well into the overdoped region of the phase diagram.

Model of the pseudogap state

We propose a phenomenological description of how the gap function should evolve when SC coherence is

lost, i.e. the pseudogap state. Since the model has fixed parameters for the SC state, we are allowed one additional parameter to ‘force’ the transition to the PG state. There is very little data on the QP spectral change, and we try only to be qualitative; no precise fit to a PG-type spectrum is done.

Recall that the T -dependant BCS gap can be written $\Delta(T) = \beta(T)\Delta(0)$, where $\beta(T)$ is a solution to the finite-temperature gap equation and which verifies $\beta(0) = 1$ and $\beta(T_c) = 0$. A numerically exact, or simple interpolation formula, can be found for $\beta(T)$. In an analogous way, we write :

$$\Delta(E) = \alpha \Delta_{PG} (1 - \beta) + \beta \Delta_{SC}(E) \quad (18)$$

where $\Delta_{SC}(E)$ is the previous gap function and β, α vary smoothly (but arbitrarily) from 1 to 0 as a function of the strength of the perturbation (temperature, magnetic field, etc.). We assume α and β vanish at T^* and T_c , respectively, see Fig. 6. The three region phase diagram is a consequence of these two parameters, while Δ_{PG} and Δ_{SC} are the characteristic zero-temperature energies. In such a way, the three states are evidently :

$$\begin{array}{lll} \beta \neq 0 & \alpha \neq 0 & \text{SC state} \\ \beta = 0 & \alpha \neq 0 & \text{PG state} \\ \beta = 0 & \alpha = 0 & \text{Normal state} \end{array}$$

In the case where Δ_{PG} is strictly identical to Δ_p of the previous section, we get the form :

$$\Delta(E) = \alpha \Delta_p + \beta \Delta_\varphi (1 - g(E)) \quad (19)$$

so that the ‘condensation amplitude’ is $\beta \Delta_\varphi$ and the ‘total’ spectral gap is $\Delta_0 = \alpha \Delta_p + \beta \Delta_\varphi$.

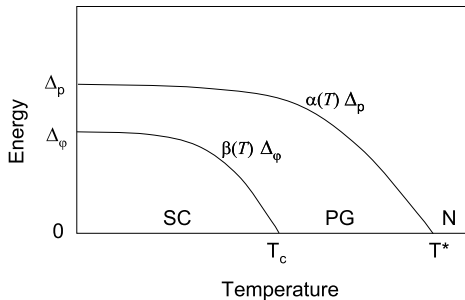


Fig. 6. Extension of the model to finite temperature showing the T -dependence of α and β .

The QP-DOS shape corresponding to the PG state is an unsolved problem, but there are many models [20, 21, 22, 23, 24, 25, 26, 27, 28, 29, 56, 57, 58, 62, 76, 77]. There is a strong indication of a broad-band self-energy in this case [7, 43, 52, 53, 57, 65]. Furthermore, as discussed in the introduction, the PG-DOS is characterized by the absence of quasiparticle peaks. Atkinson et al. [21, 65] have extended the earlier work of Huscroft & Scalettar [57] that a non-condensed Bose state produces a peak-less pseudogap in the DOS. This

has recently been applied to the case of spatial disorder [21]. Franz & Millis [18], in an altogether different approach, have found a pseudogap due to spontaneous currents, also typical of a fluctuating pair system.

Our exceedingly simple model is to consider Δ_{PG} with a finite imaginary part :

$$\Delta_{PG} = \Delta_p (1 - i\delta') \quad (20)$$

and to use Eq. (18) for the gap function. With β lowered from 1 to 0, the SC quasiparticle DOS evolves smoothly into the PG shape (see Fig. 7a). This type of DOS modification is seen in the STS experiment as the tip is scanned within the vortex core [12, 39, 59]. It is also seen as the effect of weak disorder [60]. Here $\delta' = .2$, which has a small, but non-negligible, influence on the energy changes previously discussed. Notice in Fig. 7a that the dip features disappear as $\beta \rightarrow 0$, along with the QP peaks.

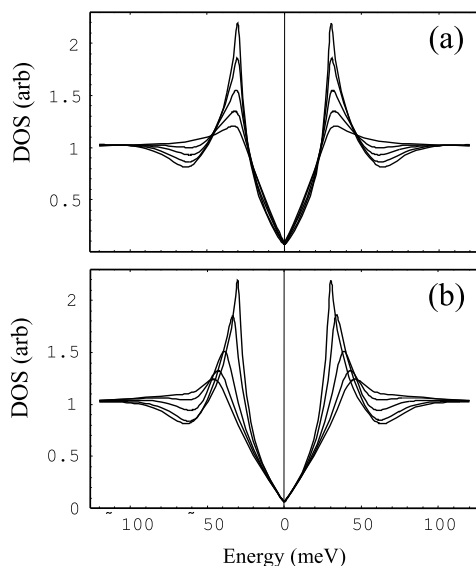


Fig. 7. Variation of the DOS with β varying from 1 (SC state) to 0 (PG state). The parameters are $p = .18$, giving $\Delta_p = 30$ meV and $\Delta_\varphi = 17.8$ meV, in Eq. 18, and $\delta' = .2$, in Eq. 20. The broadening parameters for the SC state are : $\delta = .06$, $\Gamma = .03 \Delta_p$. In (a) $\text{Re } \Delta_{PG} = \Delta_p$, in (b) $\text{Re } \Delta_{PG} = 40$ meV, i.e. larger than Δ_p .

These variations simulate the loss of SC coherence in the case (a) in the vortex core [12, 59] and (b) due to strong disorder [34, 35, 61].

In Fig. 7b we let β vanish but here $\text{Re } \Delta_{PG} > \Delta_p$: the pseudogap is slightly larger than the quasiparticle peak energy (40 meV as compared to 30 meV). Now the QP peaks move progressively out to a higher energy, as expected from Eq. (18), while being attenuated. This particular evolution is strikingly similar to STS observations [34, 35, 36, 61], and is generally attributed to disorder (inhomogeneity). In our model, the decrease of doping level on the local scale could give this effect, the result being a wider pseudogap. It corresponds to the progressive lowering of the p -value in the phase diagram of Fig. 4a. However, a disorder

potential is expected to directly affect the SC amplitude, hence $\text{Re } \Delta_{PG}$ could vary in different regions of the surface [61]. Consequently, the SC state to PG state transition energy depends on the local change of the precursor gap, $(\text{Re } \Delta_{PG} - \Delta_p)$, and on Δ_φ . An estimate of this energy is given in the following section.

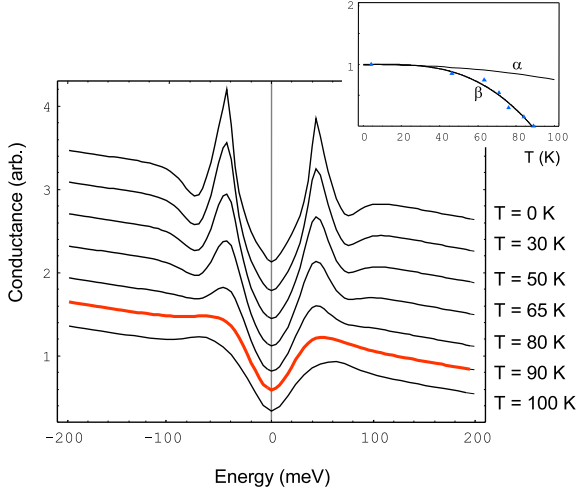


Fig. 8. Simulation of the tunneling conductance with temperature. The value of β , varying from 1 (SC state) to 0 (PG state), was inferred from the data [54], shown in the upper inset. The parameters are $p = .14$, giving $\Delta_p = 42$ and $\Delta_\varphi = 17.6$ meV, in Eq.18. All other parameters are the same as in Fig.7a. Here we assume $\text{Re } \Delta_{PG} = \alpha \Delta_p$ where α decreases slightly from unity (see inset). The highlighted spectrum corresponds to T_c .

The well-known experiment of Renner et al. [54] gives the quasiparticle conductance spectrum as a function of rising temperature. In Fig. 8 we plot a simulation of the temperature dependance of the QP spectra using Eqs. (4, 9) and the gap function (19). The standard broadening of $N_S(E)$ due to Fermi statistics is taken into account [74]. The value of $\beta(T)$ is inferred from the data (upper inset, Fig. 8) and it vanishes at $T_c \simeq 89$ K. The p value is chosen such that $\Delta_p(p) \simeq 42$ meV. As is well established from many experiments, the PG persists well above T_c , up to the temperature T^* previously discussed. Our model, as shown in Fig. 8, gives a simple qualitative description of the QP DOS with rising temperature.

III. INTERPRETATION OF THE ENERGIES

We turn to the question of interpreting the two energy scales (Δ_p , Δ_φ) that are the main ingredients of the gap function $\Delta(E)$, as expressed in (19). The foregoing work shows that, for large QP energies and along the anti-nodal direction, the total spectral gap is $\Delta(E) \simeq \Delta_0 = \Delta_p + \Delta_\varphi$, where Δ_p defines the QP peak positions, and the new parameter, Δ_φ , is proportional to $T_c(p)$. We now consider the energy changes involved in both the normal to SC and the PG to SC transitions. In the latter case we use (20) for the PG

gap, with the assumption: $\text{Re } \Delta_{PG} = \Delta_p$, with a small imaginary part.

Consider first the BCS case of a constant isotropic gap of value Δ in the SC spectrum. The approximate change in energy is given by the familiar integral:

$$\begin{aligned} (E_N - E_{SC})_{BCS} &= N_n(0) \int_0^{2\pi} \frac{d\theta}{2\pi} \int d\epsilon_k \left(\frac{\epsilon_k^2}{E_k} - |\epsilon_k| \right) \\ &+ N_n(0) \int_0^{2\pi} \frac{d\theta}{2\pi} \int d\epsilon_k \frac{\Delta}{2 E_k} \end{aligned} \quad (21)$$

The first and second terms [78] are the change in kinetic and potential energies, respectively, while the variation of the chemical potential is neglected. The high energy cut-off is unnecessary since the integrand vanishes faster than $1/\epsilon_k$. The standard result is:

$$(E_N - E_{SC})_{BCS} = \frac{1}{2} N_n(0) \Delta^2$$

or equivalently, putting $N_p = N_n(0)\Delta/2$ as the number of pairs,

$$\frac{(E_N - E_{SC})_{BCS}}{N_p} = \Delta \quad (22)$$

The conventional interpretation is therefore straightforward: the gap in the QP spectrum is equivalent to the energy gain per pair in the $N \rightarrow SC$ transition. The latter intensive quantity is related to the mean-field critical temperature, $\Delta = 1.76 k_B T_c^{MF}$.

In the unconventional case, we must go beyond the mean-field due to three possible effects (a) weak phase-stiffness and 2D electronic structure (Kosterlitz-Thouless limit), (b) proximity to Bose-Einstein condensation and (c) coupling to a collective mode (additional degrees of freedom). Denoting E_φ the energy gain due to one of these processes:

$$(E_N - E_{SC}) = (E_N - E_{SC})'_{BCS} + E_\varphi$$

where $(E_N - E_{SC})'_{BCS}$ is given by (21), but using the complete gap function $\Delta(E_k)$ (i.e. an extended BCS energy). The latter is calculated by using (18), with $\alpha = \beta = 1$, and integrating (21):

$$(E_N - E_{SC})'_{BCS} \simeq \frac{1}{2} \times \frac{1}{2} N_n(0) \Delta_p^2$$

where the extra factor of $1/2$ is from the angular integral for the d -wave case. Here one would have expected a *higher gap value* than Δ_p (between Δ_p and Δ_0), but the anti-resonant shape of $\Delta(E)$ leads to this simple result and is discussed below. The total energy change from the normal to SC states is then:

$$(E_N - E_{SC}) = \frac{1}{4} N_n(0) \Delta_p^2 + E_\varphi \quad (23)$$

If one estimates the new number of gapped pairs as $N_p = N_n(0)\Delta_p/2\sqrt{2}$, dividing through by N_p gives:

$$\frac{(E_N - E_{SC})}{N_p} = \frac{1}{\sqrt{2}} \Delta_p + \frac{E_\varphi}{N_p} \quad (24)$$

This equation matches our expression: $\Delta_0 = \Delta_p + \Delta_\varphi$, with the identification:

$$\frac{1}{\sqrt{2}}\Delta_0 = \frac{(E_N - E_{SC})}{N_p} \quad \text{and} \quad \frac{1}{\sqrt{2}}\Delta_\varphi = \frac{E_\varphi}{N_p} .$$

Neglecting the small imaginary part of Δ_{PG} , we find the energy change (N \rightarrow PG):

$$\frac{(E_N - E_{PG})}{N_p} = \frac{1}{\sqrt{2}}\Delta_p \quad (25)$$

and finally, combining (23) and (24),

$$\frac{(E_{PG} - E_{SC})}{N_p} = \frac{E_\varphi}{N_p} \quad (26)$$

Thus the E_φ term is precisely the energy gain of the SC state with respect to the PG state: the condensation energy. The intensive quantity, E_φ/N_p , is of the order of $k_B T_c$. Since E_φ is not a ‘pairing’ energy, we put $N_p = N/2$ and obtain:

$$\Delta_\varphi = 2\sqrt{2} \frac{E_\varphi}{N} \simeq 2\sqrt{2} k_B T_c \simeq 2.8 k_B T_c$$

in qualitative agreement with the fits. We have thus shown that the heuristic parameter Δ_φ is consistent with a condensation energy, E_φ , going beyond the BCS mean-field value.

These arguments cannot prove whether Δ_p is a pairing gap (pre-formed pairs above T_c) or a competing order gap (spin density wave, etc.). It is compatible with many models where states, in the energy range $\sim \Delta_p$, are first removed at the Fermi level. However, our model suggests that the new quantity, $\Delta_\varphi = 2\sqrt{2} E_\varphi/N$, is not the opening of a second gap at the SC transition. Indeed, in a first approximation, the total change in KE & PE (i.e. given by the BCS Eq. (21)) is identical with the pseudogap contribution:

$$(E_N - E_{SC})'_{BCS} \simeq (E_N - E_{PG}) \quad (27)$$

with the consequence:

$$(E_{PG} - E_{SC})'_{BCS} \simeq 0 \quad (28)$$

However, as previously noted, this is compatible with experiment: using STS, the PG width measured at the vortex core is about the same magnitude as the SC gap between the vortices. The condensation energy term, $E_\varphi = (E_{PG} - E_{SC})$, is therefore apart, and must be due to additional degrees of freedom beyond the mean field.

Behind these results (26-28) is a non-trivial movement of states in the PG \rightarrow SC transition [63]. Consider again Fig. 3 plotting the shape of the gap function, and in particular, the role of Δ_φ . The states at higher energy, $E \gg E_{dip}$, are removed ($\Delta(E) \sim \Delta_p + \Delta_\varphi$) while they are added near the anti-resonance ($\Delta(E_0) \sim \Delta_p - \Delta_\varphi$). Due to a detailed balance of energy states in the integrand $f(\epsilon_k)$ of (21), the effect

cancels out and we are left with the result Eq. (27). This is explicit in Fig. 9 where $f(\epsilon_k)$ is plotted as a function of ϵ_k (along $\theta = 0$). We use the previous gap expression with $\alpha = 1$:

$$\Delta(E_k) = \Delta_p + \beta \Delta_\varphi (1 - g(E_k))$$

and we compare directly the cases of $\beta=1$, and $\beta=0$. As expected, the latter curves cross in such a way as the subtended areas are the same. In our view, this removal of states at higher energy, also seen in the spectral function (Sec. IV), is a significant aspect of the problem. A microscopic theory should arrive at a clear dependence of E_φ on this effect.

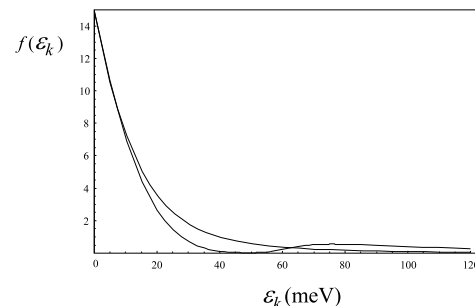


Fig. 9. Plot of the integrand, $f(\epsilon_k)$, of the BCS energy equation (21) in units of $N_n(0)/(2\pi)$ and for $\theta = 0$. The two curves compare the case of a constant gap, with $\Delta_p = 30$ meV ($p = .18$), with the case of the gap function, from Fig. 3. The latter curve shows a pronounced dip - hump feature, but the subtended areas are the same.

It is possible that, in some instances, the pseudogap is larger than the QP peak position: $\Delta_{PG} > \Delta_p$. The total energy change, Eq. (23), remains valid but (26) becomes:

$$(E_{PG} - E_{SC}) = -\frac{1}{4}N_n(0)(\Delta_{PG}^2 - \Delta_p^2) + E_\varphi$$

The change in gap value now opposes the previous condensation energy term. (In fact, if Δ_{PG} is large enough, then no transition to the SC state occurs: the above vanishes identically.) A disorder potential could be such a cause, when amplitude fluctuations are expected. Then, the above equation implies a change in the number of gapped states at the PG \rightarrow SC transition and, in this case, E_φ need not strictly be the order parameter.

The question for further work is to interpret the condensation amplitude, $\Delta_\varphi = 2\sqrt{2} E_\varphi/N$. A likely candidate is the phase stiffness J relevant to the Kosterlitz-Thouless (KT) transition:

$$E_\varphi/N = (\pi/2)J = k_B T_c^{KT}$$

For free-electrons in two dimensions, one shows that [62]: $J = n\hbar^2/4m$, the main point being that $J \propto n$, the particle density. From the previous fits to the data, we inferred that $\Delta_\varphi = (p/2p_0)\Delta_p$, so that it is at least proportional to the excess density p . If the KT

mechanism is involved, then the principal quantity of the SC gap function is predicted to be :

$$\Delta_\varphi = \sqrt{2} \pi J = 2\sqrt{2} k_B T_c^{KT}$$

with a new condition on the phase-stiffness :

$$\sqrt{2} \pi J = \frac{p \Delta_p}{2 p_0}$$

The latter result is satisfactory; the phase rigidity is now proportional to both the carrier density and the precursor interaction. Put another way, using $p' \propto N_n(0) \Delta_p$ as the density of gapped states, we have the simple constraint: $J \propto p p'$. Since the latter is valid for all p (ranging from 0 to $2p_0$), the dome-shaped SC phase diagram is obtained, i.e. $p p' \propto T_c(p)$.

In summary, without committing to a specific camp in the high- T_c problem, the total spectral gap is $\Delta_0 = \Delta_p + \Delta_\varphi$, where Δ_p is the precursor gap and the amplitude Δ_φ is proportional to the condensation energy. The latter term, and its link to the phase diagram, points however to the mechanism of ‘pre-formed’ pairs followed by KT condensation. This situation of two energy scales was suggested in the work of G. Deutscher [79], where the QP tunneling gap (Δ_p) is distinct from the coherence gap (Δ_φ ?) as inferred by the Andreev effect.

Further comments on the gap function

Consider the question of why the particular QP spectrum, $E_{\mathbf{k}}$, with the anti-resonant gap function $\Delta(E_{\mathbf{k}})$, is needed to produce the correct QP-DOS. First, the resonance is shown to cause a shift in the quasiparticle states, at the PG to SC transition, from higher energy to lower energy, manifested by the sharp QP peaks and dip features. Nevertheless, a simple answer for the energy change is obtained. All these points indicate that the condensate itself is non-trivial [63]. Furthermore, the new quantity Δ_φ enters the resonance position ($E_0 \simeq \Delta_0$), its width and its amplitude ($2\Delta_\varphi$); a property shown to be empirically correct throughout a wide doping range. Then it seems unlikely that the resonance is due to the coupling to a quasi-independent collective mode. In the latter case, the width of the resonance would reflect the collective mode damping, while its amplitude, the strength of the coupling. Here these parameters are related to the coherence amplitude, $\Delta_\varphi \propto E_\varphi/N$, possibly tied to the phase-stiffness J , and hence to the condensate itself.

The reason for the energy dependence of the gap function is so far unknown from first principles. Aside from strong-coupling theory [3], an E dependent gap appears in McMillan’s proximity effect [80], two-band superconductivity [81], and the asymmetric particle-hole case [47]. However, a highly relevant example is the detailed work of [82] on the cross-over from BCS to Bose-Einstein condensation; but the gap has no resonance effect there.

The detailed form of the gap function, or self-energy as in Section IV, represents a novel pairing interaction. It is possible that there is a strong feedback effect between the precursor state, with gap Δ_{PG} , and the freezing of phase fluctuations, of amplitude Δ_φ . Then there is a complete renormalization of the gap function $\Delta(E_k)$, where E_k is the ‘exact’ quasiparticle spectrum (final state). The effect is strong enough so that if $E_k \simeq \Delta_0$, the pairing energy is reduced, $\Delta \simeq \Delta_p - \Delta_\varphi$, compared to the low-energy value $\Delta \simeq \Delta_p$. On the contrary, at higher energy, the interaction is strong $\Delta \simeq \Delta_p + \Delta_\varphi$. This type of variation is at the heart of the QP-DOS shape.

IV. SPECTRAL FUNCTION

A different, yet equivalent, view of the same problem is given by the spectral function, $A(\mathbf{k}, E)$. It is more fundamental since there is no sum over momenta, hence an ideal quasiparticle with wave-vector \mathbf{k} is directly a Dirac peak at the position $E = E_{\mathbf{k}}$. It is also the fundamental quantity describing the ARPES measurement.

Here we discuss $A(\mathbf{k}, E)$ as given by equation (8), with the quasiparticle dispersion (7), the total gap function :

$$\Delta(E_{\mathbf{k}}) = \alpha \Delta_{PG} (1 - \beta) + \beta \Delta_{SC}(E_{\mathbf{k}})$$

and with $\Delta_{SC}(E_{\mathbf{k}})$ the usual resonant form given in (10). The gap broadening parameters are as in Sec. II, i.e. $\Delta_p \rightarrow \Delta_p (1 - i\delta)$ and $\Delta_{PG} \rightarrow \Delta_p (1 - i\delta')$ in Δ_{SC} and Δ_{PG} , respectively. The final broadening parameter is Γ_{Dynes} , and all three have been determined by the fits in Sec. II.

Since $A(\mathbf{k}, E)$ is calculated along the real ϵ_k axis, it follows that our dispersion law $E_{\mathbf{k}} = E_{\mathbf{k}}(\epsilon_k)$, Eq. (7), is complex. Considering the anti-nodal direction, the simple model gives :

$$A(\mathbf{k}, E) = \frac{1}{\pi} \frac{Im E_{\mathbf{k}}}{(E - Re E_{\mathbf{k}})^2 + Im E_{\mathbf{k}}^2} \quad (29)$$

which has the expected Lorentzian form with a peak at $Re E_{\mathbf{k}} = E$ and half-width $Im E_{\mathbf{k}}$. Such an expression neglects many-body effects that are important at higher energy [7, 15].

The spectral function (29) is presented in grey scale in Fig. 10 in the (E, ϵ_k) plane and for the case where $p = .18$. Note that the gap function is an explicit function of the QP energy, $E_{\mathbf{k}}$, and not ϵ_k ; thus one must first find numerically the (complex) dispersion law $E_{\mathbf{k}}(\epsilon_k)$ in order to apply (29). On the lower panel of Fig. 10 we give the spectral function for the SC state and compare directly with the one for the PG state (upper panel). For the SC state, the visibly sharp peak position describes a continuous curve that deviates significantly from the BCS hyperbolic law. The hyperbolic case is seen in the upper panel, since it is

inherent in the model for the pseudogap. For small ϵ both curves begin near the gap value $E \sim \Delta_p = 30$ meV, as expected. The QP peak position (SC state) begins (at P) with a slightly smaller slope than the BCS case and nearly reaches the $E = \epsilon_k$ diagonal. This is followed by a sharp kink (near $\epsilon_k = 60$ meV, at D) before joining the expected asymptote for a gap value of $\Delta_0 \simeq 48$ meV. All of these effects are totally absent in the BCS framework.

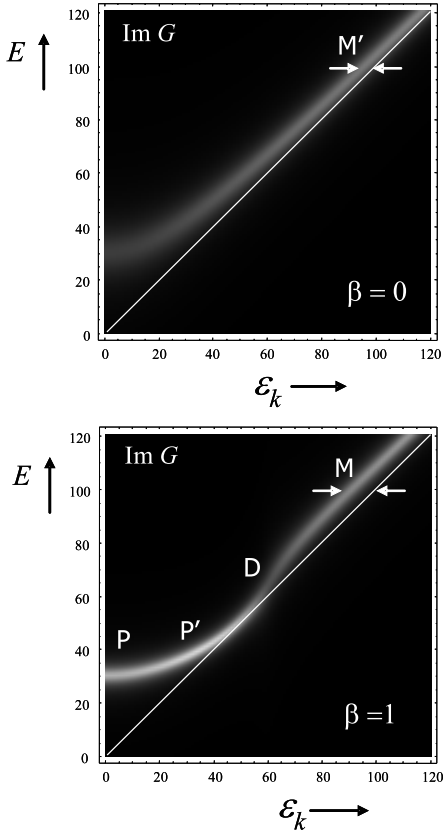


Fig. 10. Direct comparison of the spectral functions of the PG state (upper panel) and of the SC state (lower panel), viewed as density plots in the (E, ϵ_k) plane. The gap parameters correspond to $p = .18$: $\Delta_p = 30$ meV and $\Delta_\varphi = 17.8$ meV. Other relevant parameters are: $\delta = .06$, $\delta' = .2$ and $\Gamma = .06 \Delta_p$.

The dispersion law, $\text{Re } E_k$, which is hyperbolic in the PG case, has a distinctive kink (at D) in the SC case, causing the dip feature in the DOS. States are removed at high energy from the PG spectral density (compare M and M'), and are added at low energy (between P and D), in the SC spectrum.

The kink feature in the dispersion law corresponds to the dip in the QP-DOS. One can read its position, D, either on the E axis or on the ϵ_k axis: in the former, $E_{\text{dip}} \sim \Delta_p + 2\Delta_\varphi \sim 64$ meV, while in the latter $\epsilon_k \sim 2\sqrt{\Delta_0\Delta_\varphi} \sim 60$ meV (taking the point of steepest slope). The anti-resonance in the gap function is revealed here by the near touching of the diagonal by the dispersion law at the energy $E \sim \Delta_0 \sim 48$ meV. (At this point $\epsilon_k \sim E$.) Concerning the peak intensity, the sharpest QP peaks are not at $\epsilon_k = 0, E = \Delta_p$ (P in

Fig. 10) but at slightly higher energy, near 40 meV (at P'). At the kink, the peak intensity drops significantly (highest broadening), giving a quite different picture of the peak to dip feature.

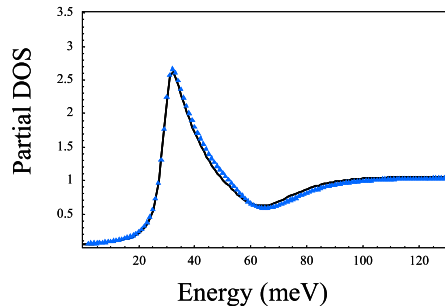


Fig. 11. Tunneling DOS (along $\theta = 0$) calculated using the exact formula (9), solid line, and the discrete sum over ϵ_k of the spectral density of Fig. 10, triangular dots.

Although ARPES can only access the occupied states, contrary to tunneling spectroscopy, the two techniques probe the same spectral function (Fig. 10). Indeed, integrating $A(\mathbf{k}, E)$ over ϵ_k , for a given E , yields the partial tunneling DOS, $n_s(E, \theta)$, as given by Eq. (6). In ARPES one can fix \mathbf{k} , hence ϵ_k , and measure $A(\mathbf{k}, E)$ as a function of E (energy distribution curve). Moreover, the dispersion of the QP states with \mathbf{k}_\parallel can be probed. Although these two techniques have different spatial and energy resolutions, it would be of high interest to establish the common spectral function that matches both the ARPES and the tunneling data.

As a simple check of the tunneling DOS, in Fig. 11 we plot both the exact partial DOS (for $\theta = 0$), using eq.(9), and the direct sum over states of the spectral density of Fig. 9. Given the crude integration method in the latter case, the agreement is satisfactory. All experimentally observed features are found: the pronounced QP peak and the dip, as well as the states within the gap from the Dynes broadening.

The upper panel of Fig. 10 shows the spectral function corresponding to the PG state, or $\beta = 0$ in the gap function, for direct comparison. Notice the significant smearing near $\epsilon_k \sim 0$, or $E \sim \Delta_p$: as expected, there are no well-defined quasiparticle peaks. The overall dispersion shape is still hyperbolic and follows $E_k \sim \sqrt{\epsilon_k^2 + \Delta_p^2}$ as imposed by the model. The asymptotic line is closer to the diagonal as compared to the SC case, where the total high-energy spectral gap is larger, i.e. $E_k \sim \sqrt{\epsilon_k^2 + \Delta_0^2}$ (compare M' with M in Fig. 10). This gives a direct view of the movement of the states in the PG \rightarrow SC transition: states well above the PG gap, for $E_k > E_{\text{dip}}$ (upper panel), are removed and a high density of quasiparticle states exist, for $E_k < E_{\text{dip}}$, in the SC state (lower panel).

Quasiparticle self-energy

The final objective of this work is to show that the E -dependant gap function is equivalent to a self-energy.

In the SC state, the carriers of energy ϵ_k are modified by the presence of $\Sigma_{\mathbf{k}}(\epsilon_k)$:

$$A(\mathbf{k}, E) = \frac{1}{\pi} \operatorname{Im} \frac{1}{E - \epsilon_k - \Sigma_{\mathbf{k}}(\epsilon_k)} \quad (30)$$

Thus, setting $\Sigma = 0$ gives the normal state spectrum, while for ideal BCS quasiparticles it is with $\Sigma_{\mathbf{k}}(\epsilon_k) = \sqrt{\epsilon_k^2 + \Delta^2} - \epsilon_k$. Finally, the Dynes lifetime broadening is obtained if Σ has an imaginary part ($\operatorname{Im} \Sigma = \Gamma$).

For the general case, where the SC state is given by the gap function, comparing (30) with our original expression (8), gives:

$$\Sigma_{\mathbf{k}}(\epsilon_k) = E_{\mathbf{k}}(\epsilon_k) - \epsilon_k \quad (31)$$

However, the final state QP energy, $E_{\mathbf{k}}(\epsilon_k)$, is a solution of the implicit equation $E_{\mathbf{k}} = \sqrt{\epsilon_k^2 + \Delta_{\mathbf{k}}(E_{\mathbf{k}})^2} + i\Gamma$, and thus an analytical expression for $\Sigma_{\mathbf{k}}(\epsilon_k)$ cannot be given. The computation of $E_{\mathbf{k}}(\epsilon_k)$ is quite straightforward, leading to the complex valued $\Sigma_{\mathbf{k}}(\epsilon_k)$ and hence to the spectral function (30). Formally, the quasiparticle resonance position is given by $\operatorname{Re} E_{\mathbf{k}} = \epsilon_k + \operatorname{Re} \Sigma_{\mathbf{k}}(\epsilon_k)$, and its width by $\operatorname{Im} E_{\mathbf{k}} = \operatorname{Im} \Sigma_{\mathbf{k}}(\epsilon_k)$. Note that using the definition of $E_{\mathbf{k}}$, and the simple expression (31), yields:

$$\Sigma_{\mathbf{k}}(\epsilon_k) = i\Gamma + \frac{\Delta_{\mathbf{k}}(E_{\mathbf{k}})^2}{E_{\mathbf{k}} - \epsilon_k + i\Gamma} \quad (32)$$

which is similar to the form considered by [7, 33]. Thus, the E -dependent gap function and the self-energy function are equivalent.

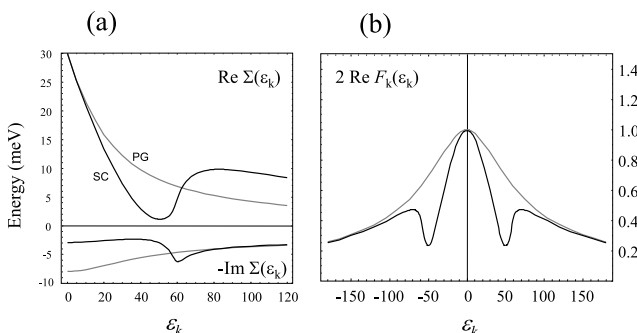


Fig. 12a. Complex self-energy plotted against ϵ_k along $\theta = 0$. Dark line - SC self-energy; gray line - PG case.

The strong dip, where $\operatorname{Re} \Sigma(\epsilon_k)$ nearly vanishes, is followed by a crossing-point with the PG line, then slowly decays at higher energy. The sudden rise in $\operatorname{Re} \Sigma(\epsilon_k)$, at a maximum of $\operatorname{Im} \Sigma(\epsilon_k)$, is at the energy $\epsilon_k \simeq 2\sqrt{\Delta_0 \Delta_{\varphi}}$, and causes the DOS dip. The sharpest QP peaks are not at $\epsilon_k \sim 0$, $E \sim \Delta_p$, but nearer ~ 40 meV.

Fig. 12b. Plot of the pair amplitude $2 F_k = \Delta_k(E)/E_k$, using the gap function (18), and compared to the BCS value, along the anti-nodal direction. (All parameters are the same as in Figs. 8-10.)

The self-energy is plotted in Fig. 12a using the same parameters as those of Figs. 10 and 11. The darker line corresponds to the SC case using the resonant gap function, the gray line is for the PG model, with a

constant gap ($\sim \Delta_p$). For small ϵ_k both curves begin at the value: $\operatorname{Re} \Sigma(0) \simeq \Delta_p \simeq 30$ meV, as expected. However, the SC curve descends sharply towards zero, as compared to the PG one, and reaches a minimum near $\epsilon_k \simeq 2\sqrt{\Delta_p \Delta_{\varphi}}$. This corresponds to the anti-resonance position in the gap function ($E = \Delta_0$). The self-energy then rises abruptly, crosses the PG reference curve and, with a further change in concavity, decays as a function ϵ_k . The dip position in the QP-DOS is found by the maximum slope of $\operatorname{Re} \Sigma(\epsilon_k)$; it is near the crossing point at $\epsilon_k \simeq 2\sqrt{\Delta_0 \Delta_{\varphi}}$. Note that this dip position coincides with the highest broadening, as revealed by $\operatorname{Im} \Sigma(\epsilon_k)$ in the lower panel of Fig. 12a. The lowest broadening is at $\epsilon_k \sim 40$ meV, giving the highest QP peaks in the spectral function, and the wide peaks seen in the DOS.

In conclusion, the self-energy of Fig. 12a is yet another way of comparing the change of states from the PG to SC cases. Indeed, the self-energy of the SC state is smaller than the PG one for small energies, up to the crossing point, when the relative magnitude inverts. Our previous observation that states are removed at large energy from the PG state, for $\epsilon_k \gg 2\sqrt{\Delta_0 \Delta_{\varphi}}$, while they are added to the SC state, for $\epsilon_k < 2\sqrt{\Delta_0 \Delta_{\varphi}}$, is seen here in a different way. The strong minimum of $\operatorname{Re} \Sigma$, near $\epsilon_k \simeq 2\sqrt{\Delta_p \Delta_{\varphi}}$, also reveals the condensation amplitude. The sharpness of these features is an indication that ARPES may be a better technique to extract these two parameters, as compared to quasiparticle tunneling.

In Fig. 12b we plot the pair amplitude $F_k = \Delta_k/2E_k$ as a function of ϵ_k [78], taking the real part. The case where the SC gap function is used is directly compared to the conventional pair amplitude, with a constant gap. The obvious dip features, near ± 50 meV, are due to the same minimum discussed previously. The investigation of this function is yet to be done in the case of cuprates; it requires the Andreev effect or pair tunneling, and not quasiparticle tunneling, in order to be probed.

V. CONCLUSIONS

Three principal questions have been addressed: does the tunneling DOS reveal the order parameter and if so, in what manner, and finally, does it connect to the phase diagram? We have tried to answer them from the heuristic point of view, i.e. by using our resonant gap function and examining the available data. This E -dependant gap produces the well-known quasiparticle peak shapes, followed by the dip structures at higher energies. No Fermi surface anisotropy, no van Hove singularity, no strong-coupling are needed; only simple d -wave quasiparticles, with a modified spectrum, are considered.

The model contains two fundamental energy scales, whose values are determined by the fits to the tunneling spectra: Δ_p , the quasiparticle peak position, and

a second energy, Δ_φ . We found the resonance (along the anti-nodal direction) to be at the fixed position $\Delta_0 = \Delta_p + \Delta_\varphi$, coinciding with the total spectral gap for high energies, i.e. $E_k \simeq \sqrt{\epsilon_k^2 + \Delta_0^2}$. Thus, the description of the SC state depends uniquely on this new energy scale: Δ_φ .

To go a step further, we showed that these two energy scales fit the phase diagram as a function of carrier density, p . While Δ_p decreases linearly with doping, Δ_φ follows T_c , with $\Delta_\varphi = 2.3 k_B T_c$, and merges smoothly with Δ_p at high doping. Thus the gap function scales perfectly with the carrier density; one can then generate the QP-DOS shape for arbitrary p . The two energy scales have a simple link: $\Delta_\varphi \propto p \Delta_p$, valid in the range of the available data. If there is a critical point, it would be at maximal doping where both energy scales vanish.

The role of Δ_φ as a new condensation amplitude is compelling. To check this, we estimated the energy changes associated with the three states (normal, PG, SC). A simple interpretation for each term of the constraint $\Delta_0 = \Delta_p + \Delta_\varphi$ is, respectively: the total energy gain (per pair), the energy gain due to the precursor gap (PG state) and the condensation energy per pair E_φ/N_p . However, the number of gapped pairs turns out to be $N_p \propto \Delta_p/2$ and *not* $N_p \propto \Delta_0/2$, which is thus in support of the preformed-pair model. For a competing order gap, N_p is to be simply taken as half the number of gapped states. In either case our new amplitude turns out to be $\Delta_\varphi = \sqrt{2} E_\varphi/N_p$. It is therefore justified, for both scenarios, that this parameter is proportional to T_c , as found independently from the fits to the data.

Since the mouvement of states in the PG to SC transition remains subtle, i.e. not the direct opening of a second (SC) gap, we took a closer look at the dispersion law $E_{\mathbf{k}}(\epsilon_k)$. We discussed the spectral function, and the corresponding self-energy, where the change of the quasiparticle states can be seen more readily than in the DOS. Indeed, it allows to identify features of the QP spectrum as a function of both E and ϵ_k . One finds that in the PG state quasiparticles of higher energy, $\epsilon_k \gg 2\sqrt{\Delta_0 \Delta_\varphi}$, end up as quasiparticle peaks at lower energy, $\epsilon_k < 2\sqrt{\Delta_0 \Delta_\varphi}$, in the SC state. The cross-over is precisely the characteristic energy where the dip feature is seen, either in the self-energy or in the gap function. By a different analysis than of the DOS, we found that this mouvement of the states depends uniquely on Δ_φ .

Our model shows that the principal change of kinetic and potential energies (as in BCS) is associated with the opening of the precursor gap $\Delta_{PG} \simeq \Delta_p$, at the Fermi level (normal state to PG state transition). At the SC transition, the quantity E_φ is therefore linked to other degrees of freedom not accounted for in the BCS model. This possibility is accentuated by the resonant character of the gap function. While a particular collective effect is perhaps responsible, a likely candidate for the condensation energy is the phase stiffness,

J , in the Kosterlitz-Thouless transition. In this context, we get an immediate relation between our parameter and J : $\Delta_\varphi = \sqrt{2\pi} J$ which is then proportional to the KT transition temperature. A relevant prediction is thus: $J \propto p \Delta_p$, should the KT mechanism fit the phase diagram, for a wide range of doping.

The three questions above have therefore been given a tentative answer. One could raise some objection to introducing an *ad hoc* gap function, where a microscopic theory is missing. Some speculations concerning the physical origin of the gap function have been given in the closing paragraphs of Sec. III. Our main goal of matching the observed experimental QP-DOS, and their characteristics as a function of the carrier density, works without resorting to additional extraneous factors. Moreover, the fits can now be done with a minimal set of parameters. Finally, the two key parameters, the QP peak position Δ_p , and the coherence amplitude Δ_φ , have been connected to observed physical quantities.

One of the authors (W.S.) thanks Amir Kohen & Th. Proslier, for interesting and helpful discussions.

- [1] J. Bardeen, L. Cooper, J. Schrieffer, Phys. Rev. **108**, 1175 (1957).
- [2] *Superconductivity*, R.D. Parks, ed. (Dekker, New York, 1969).
- [3] J.R. Schrieffer, Rev. Mod. Phys. 200, (1964), and J.R. Schrieffer, *Theory of Superconductivity*, (W.A. Benjamin, New York, 1964).
- [4] I. Giaever, Phys. Rev. Lett. **5**, 147 (1960).
- [5] W.Y. Liang, J. Phys. Condens. Matter **10**, 11365 (1998) and T. Timusk and B. Statt, Rep. Prog. Phys. **62**, 61 (1999);
- [6] J. Tallon and J. Loram, Physica C **349**, 53 (2001).
- [7] M. Norman, M. Randeria, H. Ding et al., Phys. Rev. B **57**, R11093 (1998);
- [8] J.C. Campuzano et al., Phys. Rev. Lett. **83**, 3708 (1999)
- [9] N. Miyakawa et al., Phys. Rev. Lett. **83**, 1018 (1999)
- [10] Ch. Renner and Ö. Fisher, Phys. Rev. B **51**, 9208 (1995).
- [11] T. Cren et al., Europhys. Lett., **52** (1), 203 (2000)
- [12] S. Pan, E. Hudson, et al., Phys. Rev. Lett. **85**, 1536 (2000).
- [13] J. Zasadzinski et al., Phys. Rev. Lett. **87**, 67005 (2001).
- [14] D. Coffey and L. Coffey, Phys. Rev. Lett. **70**, 1529 (1993).
- [15] M. Norman and H. Ding, Phys. Rev. B **57**, R11089 (1998);
- [16] P. Monthoux et D. Pines, Phys. Rev. B **49**, 4261 (1994); P. Monthoux, A. Balatsky et D. Pines, Phys. Rev. B **46**, 14 803 (1992)
- [17] M. Eschrig and M. Norman, Phys. Rev. Lett. **85**, 3261 (2000).
- [18] M. Franz and A.J. Millis, Phys. Rev. B **58**, 14572 (1998).
- [19] P. W. Anderson *The Theory of Superconductivity in the high- T_c Cuprates*, (Princeton Univ. Press, New

Jersey, 1997).

[20] A.J. Millis, Physica B **312**, 1-6 (2002).

[21] W. A. Atkinson, Phys. Rev. B **71**, 24516 (2005).

[22] Ar. Abanov, A. Chubukov and J. Schmalian, cond-mat 0010403

[23] F. Ohkawa, Phys. Rev. B **69**, 104502 (2004).

[24] V. Emery et S. Kivelson, Nature **374**, 434 (1995).

[25] H.-J. Kwon, A. Dorsey and P. Hirschfeld, Phys. Rev. Lett. **86**, 3875 (2001).

[26] V. Loktev, R. Quick, S. Shaparov, Phys. Rep. **349**, 1 (2001), and refs. therein.

[27] M. Vojta, Y. Zhang, S. Sachdev, Phys. Rev. Lett. **85**, 4940 (2000). C. Castellani, C. Di Castro, and M. Grilli, Phys. Rev. Lett. **75**, 4650 (1995).

[28] S. Chakravarty, R. Laughlin et al., Phys. Rev. B **63**, 94503 (2001).

[29] C. Varma, Phys. Rev. B **55**, 14554 (1997).

[30] K. Levin, Q. Chen, I. Kosztin et al., J. Phys. Chem. Sol. **63**, 2233 (2002).

[31] J. Zasadzinski et al., Phys. Rev. Lett. **96**, 17004 (2006).

[32] J. Zasadzinski et al., Phys. Rev. B **68**, 180504 (2003).

[33] B. Hoogenboom et al., Phys. Rev. B **67**, 224502 (2003).

[34] C. Howald, P. Fournier and A. Kapitulnik, Phys. Rev. B **64**, 100504 (2001).

[35] S. Pan, J. P. O'Neal, R. L. Badzey et al., Nature **413**, 282 (2001).

[36] A. Sugimoto, S. Kashiwaya, H. Eisaki et al., (preprint).

[37] Z. Wang, J.C. Girard et al., *STM and Related Techniques : 12th Int. Conf.*, Amer. Inst. of Phys. (2003).

[38] Y. Xuan, H. Tao, Z. Li et al., cond-mat 0107540.

[39] K. Matsuba et al., J. Phys. Soc. Jap. **72** 2153 (2003).

[40] A. Fang et al., Phys. Rev. Lett. **96**, 017007 (2006).

[41] Ar. Abanov and A. Chubukov, Phys. Rev. Lett. **83**, 1652 (1999).

[42] Ar. Abanov, A. Chubukov and J. Schmalian, Europhys. Lett. **55**, 369 (2001).

[43] A. Chubukov and D. Morr, Phys. Rev. Lett. **81**, 4716 (1998).

[44] Y. Bang and H.-Y. Choi, Phys. Rev. B **62**, 11736 (2000).

[45] A. Abrikosov, Physica C **341**, 97 (2000).

[46] Z. Yusof, J. Zasadzinski, L. Coffey and N. Miyakawa, Phys. Rev. B **58**, 514 (1998).

[47] J. E. Hirsch, Phys. Rev. B **59**, 11 962, (1999)

[48] D. van Harlingen, Rev. Mod. Phys. **67**, 515 (1995).

[49] H. Ding, J.C. Campuzano, M. Norman et al., J. Phys. Chem. Solids **59**, 1888 (1998).

[50] H. Ding et al., Nature **382**, 51 (1996).

[51] A. Loeser et al., Science **273**, 325 (1996).

[52] M. Norman et al., Phys. Rev. Lett. **79**, 3506 (1997);

[53] A. Kaminsky et al., Phys. Rev. Lett. **84**, 1788 (2000).

[54] Ch. Renner et al., Phys. Rev. Lett. **80**, 149 (1998).

[55] R. Markiewicz, *comment*, Phys. Rev. Lett. **89**, 229703 (2002).

[56] J. Maly, B. Jankó, and K. Levin, Phys. Rev. B **59**, 1354, (1999).

[57] C. Huscroft and R. Scalettar, Phys. Rev. Lett. **81**, 2775 (1998).

[58] A. Ghosal, M. Randeria and N. Trivedi, Phys. Rev. B **63**, 20505 (2000).

[59] Ch. Renner et al., Phys. Rev. Lett. **80**, 3606 (1998).

[60] T. Cren, D. Roditchev, W. Sacks et al., Phys. Rev. Lett. **84**, 147 (2000).

[61] T. Cren, D. Roditchev, W. Sacks et al., Europhys. Lett., **54** (1), 84 (2001).

[62] P. Nozières and F. Pistoletti, Eur. Phys. J. B **10**, 649 (1999).

[63] M. Norman, M. Randeria et al. Phys. Rev. B **61**, 14742 (2000)

[64] E. Hudson et al., Science **285**, 88 (1999); A. Yazdani et al., Phys. Rev. Lett. **83**, 176 (1999).

[65] W. Atkinson, P. Hirschfeld and A. MacDonald, Phys. Rev. Lett. **85**, 3922 (2000).

[66] H. Kruis, I. Martin, and A. V. Balatsky, Phys. Rev. B **64**, 54501 (2001); B. Andersen, A. Melikyan et al., Phys. Rev. Lett. **96**, 97004 (2006).

[67] B. Hoogenboom et al. Physica C **391**, 376 (2003);

[68] Ph. Bourges et al. Physica C **424**, 45 (2005) and refs. therein.

[69] P. Mallet et al., Phys. Rev. B **54**, 13324 (1996).

[70] S. Matsuura et al., Physica C **300** 26 (1998).

[71] E. L. Wolf *Principles of Electron Tunneling Spectroscopy*, (Oxford Univ. Press, 1985).

[72] H. Won and K. Maki, Phys. Rev. B **49**, 1397 (1994).

[73] R. C. Dynes, V. Narayanamurti, and J. P. Gorno, Phys. Rev. Lett. **41**, 1509 (1978)

[74] N. Bergeal, V. Dubost et al., cond-mat 0604208.

[75] A. Kohen, Th. Proslier et al., cond-mat/0511699.

[76] A.A. Abrikosov, Phys. Rev. B **63**, 134518 (2001).

[77] F. Fistulo de Abreu and B. Douçot, Phys. Rev. Lett. **86**, 2866 (2001)

[78] P. G. de Gennes *Superconductivity of Metals and Alloys*, (W.A. Benjamin, New York, 1966).

[79] G. Deutscher, Nature **397**, 410 (1999).

[80] W. L. McMillan, Phys. Rev. **175**, 537 (1968).

[81] H. Suhl, B. T. Matthias, and L. R. Walker, Phys. Rev. Lett. **3**, 552 (1959).

[82] P. Nozières and S. Schmitt-Rink, J. Low Temp. Phys. **59**, 195 (1995).